Similarities in Dielectrophoretic and Electrophoretic Traps

Nichith CHANDRASEKARAN [1], Ramki MURUGESAN [1], Jae Hyun PARK [2,3,*]

* Corresponding author: Tel.: +82 (0)55 772-1585; Fax: +82 (0)1895 256392; Email: parkj@gnu.ac.kr
1 School of Mechanical and Aerospace Engineering, Gyeongsang National University, South Korea
2 Department of Aerospace and System Engineering, Gyeongsang National University, South Korea
3 Research Center for Aircraft Parts Technology, Gyeongsang National University, South Korea

Abstract In this study we present a universal theoretical formulation of the particle motions in electrophoretic and dielectrophoretic traps. It is extended from the well-known Mathieu equation based theories for Paul trap. The white noise random force model is utilized to form the Brownian motion of particle in the traps and the instantaneous dielectrophoretic force is employed rather than the time-averaged ponderomotive expression. The new approach enables many interesting properties of dielectrophoretic traps about stability and random motion. This study will be expected to provide a concrete protocol for the design of nanoscale traps which is essential in single molecule analysis.

Keywords: Dielectrophoretic trap, Paul trap, Random motion, Universality

1. Introduction

Electrpohoresis (EP) and Dielectrophoresis (DEP) are two representative object-manipulation principles used in various biological applications including trapping, sorting, separation of cells, viruses, nanoparticles, etc. (Hughes and Morgan, 1998; Hughes, 2000; Voldman et al., 2006, Guan et al., 2011; Park et al., 2012). EP is the motion of charged particles due to the electric field by following Columbic law while DEP is the movement of the suspended particles in solvent resulting from polarization forces induced by an inhomogeneous electric field. Due to the difference in fundamentals, DEP is usually applied to the neutral particles while EP is utilized to handle the charged particles.

In the present study, we consider the planar quadrupole dielectrophoretic trap (planar QDT, see Figure 1), in which four electrodes are aligned mutually perpendicular and pointing towards the trap center. Oscillating (AC) electric fields are applied to the electrodes such that the phase angle of the field between adjacent electrodes is 180°. Such geometrical configuration is same as that of planar Paul trap (planar PT) which is typically used to trap the charged atom and ions in low pressure environment (Hughes, 2000).

Although both planar QDT and PT employ the quadrupole electrodes with AC field, their

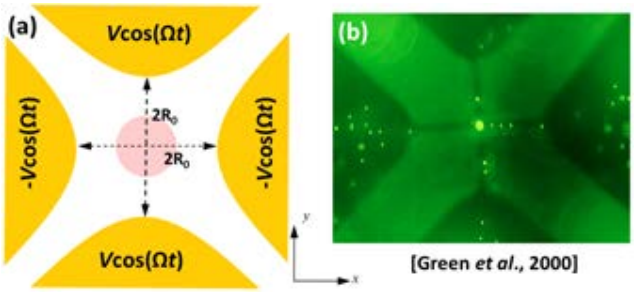

Figure 1 (a) Schematic of quadrupole Paul/dielectrophoretic traps; (b) Trapping of sub-micro particles with quadrupole dielectrophoretic trap (experiment) [Huges et al, 1998]

analyses are quite different: For DEP traps, people have mostly been interested in the static characteristics, which is governed by the ponderomotive components. However, for PT the rigorous understanding of dynamic features (e.g. stability) including static ones has been established with the aid of Mathieu function theory. It enables an accurate estimation of particle random motion at long-time limit.

Conventionally, the stability of DEP trap has been known to be determined by the sign

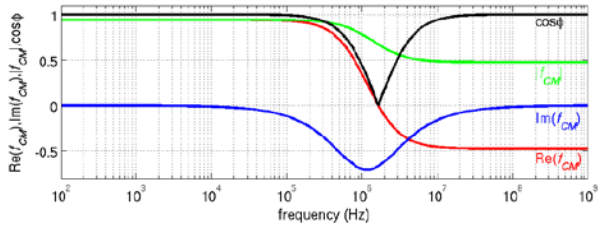

Figure 2. Clausius-Mossotti factor for the polystyrene beads in water. Their dielectric constant is ϵ_p = 2.55, and electric conductivity is σ_p = 0.01 S/m. The dielectric constant of de-ionized water is ϵ_m = 78.5 and the conductivity is $\sigma_m = 1 \times 10^{-5}$ S/m.

of real part of Clausius-Mossotti factor, $f_{CM} = (\tilde{\varepsilon}_p - \tilde{\varepsilon}_m)/(\tilde{\varepsilon}_p + 2\tilde{\varepsilon}_m)$, where $\tilde{\varepsilon} = \varepsilon - (\sigma / j\omega)$, ε is the product of dielectric constant of material and vacuum permittivity (ε_o = 8.854×10−12 F/m), σ is electric conductivity, j is the imaginary unit, $j = \sqrt{-1}$, ω is AC frequency. The subscripts p and m indicate particle and medium, respectively. Re(f_{CM}) has the value of $\frac{\sigma_p - \sigma_m}{\sigma_p + 2\sigma_m}$ at low frequency limit ($\omega \rightarrow 0$) and $\frac{\varepsilon_p - \varepsilon_m}{\varepsilon_p + 2\varepsilon_m}$ at high frequency limit ($\omega \rightarrow \infty$) (see Figure 2). Re($f_{CM}$) becomes zero at the critical frequency of $\omega_{crit} = \sqrt{(\sigma_p - \sigma_m)(\sigma_p + 2\sigma_m)/((\varepsilon_m - \varepsilon_p)(\varepsilon_p + 2\varepsilon_m))}$. If the particle is less polarizable than the medium ($\omega > \omega_{crit}$), then Re(f_{CM}) becomes negative, and the particles experience the force towards field minima (negative DEP, or nDEP). If the relative polarizability is greater than that of the medium ($\omega < \omega_{crit}$), then Re(f_{CM}) will be positive (positive DEP, or pDEP), and the particle moves to field maxima (Voldman, 2006). In PQDT, nDEP makes the trap stable by localizing the targets towards the center, whereas pDEP pushes the particles towards the electrodes and the trap becomes unstable.

At low AC field frequencies, the ions have enough time to follow each change in sign of the field direction, so the conductivity effect is dominant. However, At high frequency the ions do not have enough time to follow the change in sign of the field. Thus the permittivity dominates (Orlin et al, 2009). The polystyrene is known as good dielectric material even at high AC frequency, so its electric conductivity can be assumed constant regardless of the change of AC frequency. The electric properties of electrolyte vary with frequency (Jones et al., 2004). However, the AC frequencies utilized in electrophoretic and dielectrophoretic traps are sufficiently high (> 100 kHz) in which the electric properties do not change any more. Considering this, the variation of electric properties with AC frequency is not included in this study.

The quadrupole electrode configuration is also used for the Paul trap (planar quadrupole Paul trap, PQPT) which traps charged particles (e.g. atoms and ions) (Paul, 1990). Although both PQDT and PQPT use the quadrupole electrodes with AC-field, their analyses are quite different from each other: The particle motions in DEP trap have been investigated with the period-averaged ponderomotive DEP force (Huges et al, 1998 and Voldman et al, 2001), whereas for PQPT the dynamics is understood based on the instantaneous electrophoretic force (Arnold et al, 1993, Hasegawa et al, 1995, Major et al, 2005 and Park et al, 2012). Such difference gives rise to the following question: Does a universal theory for the electrical traps exist? Also, the random motion in DEP trap has not been attracted so far possibly because the DEP usually traps the micro-objects whose size is sufficiently larger than the thermal noise. However, if the size of particle is in nanoscale, its random motion becomes prominent. The current rapid development of single molecule analysis (Gupta, 2008 and Walter et al, 2008) highly demands the trapping of nanometer- and/or sub-nanomoter-sized biological objects (DNA, proteins, etc.).

Considering all the above, in this study we employ the equation of motion (EOM) with instantaneous DEP force, and then investigate the stabilities in analogue with the theories for PQPT. Also, the random fluctuations in PQDT are rigorously examined.

2. Equation of Motion (EOM)

EOM for the particles in EP trap (x-direction) is given by:

$$m\frac{d^2x}{dt^2} = -\gamma\frac{dx}{dt} + F_{DEP,x} + \sqrt{2k_BT\gamma}W(t) \qquad (1)$$

where γ is the viscous friction coefficient formulated as $\gamma = 6\pi\eta r$. r is the particle radius and η is the medium viscosity. $\sqrt{2k_BT\gamma}W(t)$ is the fluctuation force due to random impulse from the neighboring fluid molecules and *W(t)* is the white noise with (mean, variance) = (0,1). The DEP force, $F_{x,DEP}$ can be expressed with the multi-pole expansion in quadrupole electric field (Washizu et al, 1996):

$$F_{DEP,x} = 2A_{DEP} \times \left[\mathrm{Re}(f_{CM}) + \left|f_{CM}\right|\cos(2\omega t - \phi)\right]x \qquad (2)$$

where

$$A_{DEP} = \frac{\pi\varepsilon_m r^3 V_0^2}{R_0^4} \quad , \qquad (3)$$

$$\left|f_{CM}\right| = \sqrt{\left[\mathrm{Re}(f_{CM})\right]^2 + \left[\mathrm{Im}(f_{CM})\right]^2} \quad , \qquad (4)$$

$$\tan\phi = \frac{\mathrm{Im}(f_{CM})}{\mathrm{Re}(f_{CM})} \quad . \qquad (5)$$

Considering the correspondence between *x*- and *y*-directional DEP forces, it is sufficient to examine the EOM in x-direction in identifying the dynamic features of PQDT. Therefore, the subscript *x* for F_{DEP} is dropped for simplicity hereafter.

As a first step to understand the dynamic features of PQDT, we consider the case without both fluidic damping and random force. i.e. The first and second terms in Eq. (1) are neglected.

3. Results and Discussion

3.1 No fluidic damping, no random motion

When the fluidic damping and random fluctuation are not considered, Eq. (1) becomes

$$m\frac{d^2x}{dt^2} - 2A_{DEP} \times \left[\mathrm{Re}(f_{CM}) + \left|f_{CM}\right|\cos(2\omega t - \phi)\right]x = 0$$

By introducing a dimensionless time of $\tau = \omega t$

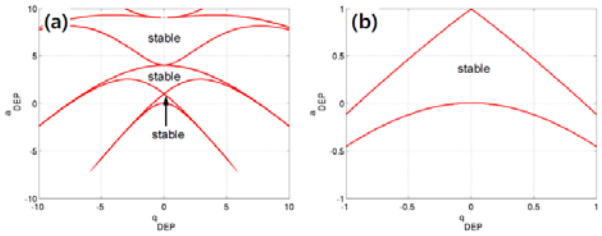

Figure 3. Stability chart for dielectrophoretic trap without fluidic damping: (a) Regular view; (b) Enlarged view near the origin

and two system parameters of $a_{DEP} = -2\frac{A_{DEP}}{m\omega^2}\mathrm{Re}(f_{CM})$ and $q_{DEP} = \frac{A_{DEP}}{m\omega^2}\left|f_{CM}\right|$, Eq. (6) can be non-dimensionalized as

$$\frac{d^2x}{d\tau^2} + \left[a_{DEP} - 2q_{DEP}\cos(2\tau - \phi)\right]x = 0 \qquad (7)$$

Now, the above expression is quite similar to the governing equation for PQPT (Mathieu equation). Although the DC field is not applied, the term mimicking DC effect naturally appears as a_{DEP} (pseudo-DC effect). This term is equivalent to the a_{PT}–parameter ($a_{PT} = \frac{2QU}{mR_0^2\omega^2}$ where U is DC voltage and Q is particle charge) expressing DC contribution to Paul trap. Due to the mathematical similarity, all the theoretical approaches for PQPT are expected to be still valid for PQDT (Paul, 1990; Major et al, 2005). Following the general procedure of the stability analysis for PQPT (Hasegawa et al, 1995) we can construct the stability chart for PQDT as illustrated in Figure 3.

For a typical micro-sized polystyrene bead (r = 1.0 μm, density is ρ_p = 1050 kg/m^3) in a micro-trap (R_0 = 4.0 μm and V_0 = 1.2 V), A_{DEP} has the value of 1.228×10^{-5} N/m. Also, a_{DEP} and q_{DEP} are expressed as $a_{DEP} = -2\frac{A_{DEP}}{m\omega^2}\mathrm{Re}(f_{CM})$ and $q_{DEP} = \frac{A_{DEP}}{m\omega^2}\left|f_{CM}\right|$, respectively. Since $\left|\frac{\varepsilon_p - \varepsilon_m}{\varepsilon_p + 2\varepsilon_m}\right| < \left|\mathrm{Re}(f_{CM})\right|, \left|f_{CM}\right| < \left|\frac{\sigma_p - \sigma_m}{\sigma_p + 2\sigma_m}\right|$ and $0 < \cos\phi < 1$, in practical applications a_{DEP} and q_{DEP} generally fulfil the condition of $\left|a_{DEP}\right| \ll 1$ and $0 < q_{DEP} \ll 1$. This condition is

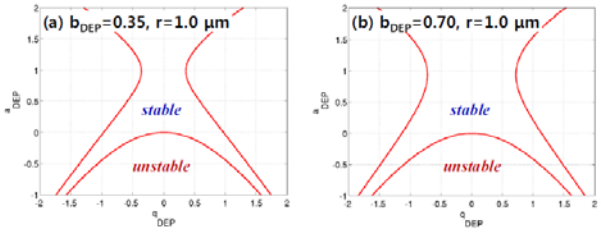

Figure 4. Stability charts for micro-particle (r=*1.0 μm*) microtrap (R_0=*4.0 μm*) with viscous medium: (a) b_{DEP} =0.35; (b) b_{DEP} =0.70.

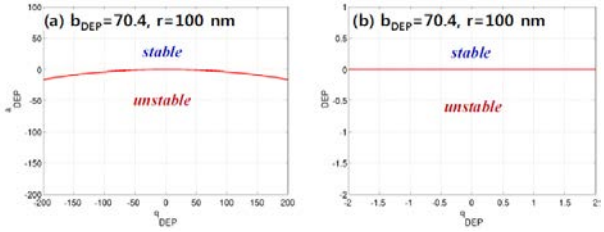

Figure 5. Stability charts for nano-particle (r=*100 nm*) microtrap (R_0=*4.0 μm*) with viscous medium: (a) b_{DEP} =0.35; (b) b_{DEP} =0.70.

valid for nano-particle in nano-trap as well, because the value of A_{DEP} is still quite small as 1.228×10^{-4} N/m for (r, R_0) = (100, 400) nm and 1.228×10^{-2} N/m for (r, R_0) = (1, 4) nm. As seen in Figure 3(b), in the very vicinity of (a_{DEP}, q_{DEP}) = (0, 0) the slope of the stability border becomes zero. It indicates that for the condition of $0< q_{DEP}\ll1$ which commonly happens in practical applications, the stability of PQDT is purely determined by the sign of a_{DEP}. The trap is stable when $a_{DEP} > 0$ and $Re(f_{CM}) < 0$ while it becomes unstable for $a_{DEP} < 0$ and $Re(f_{CM}) > 0$. This is exactly identical to the well-known conventional stability condition that PQDT is stable when $\omega > \omega_{crit}$ while it becomes unstable when $\omega < \omega_{crit}$.

3.2 With fluidic damping, no random motion

If we consider the fluidic damping without random force, Eq. (1) is expressed as

$$m\frac{d^2x}{dt^2}+\gamma\frac{dx}{dt}-2A_{DEP}\times\left[\mathrm{Re}(f_{CM})+\left|f_{CM}\right|\cos(2\omega t-\phi)\right]x=0 \tag{8}$$

In order to non-dimensionalize Eq. (8), a parameter $b_{DEP}=\frac{\gamma}{m\omega}$ needs to be introduced in addition to a_{DEP} and q_{DEP}:

$$\frac{d^2x}{d\tau^2}+b_{DEP}\frac{dx}{dt}+\left[a_{DEP}-2q_{DEP}\cos(2\tau-\phi)\right]x=0 \tag{9}$$

Figure 4 shows the stability chart for the micro-particle (r = 1μm) in the micro-trap (R_0= 4μm) with viscous medium. The b_{DEP} values in the figure are typical ones for the micro-traps. With inclusion of viscous damping, the stable area is enlarged and it further widens with increase in b_{DEP}. However, near (a_{DEP}, q_{DEP}) = (0,0), the tangent of stability border is still zero. It indicates that the stability condition of PQDT is not affected by the medium viscosity: stable with $\omega > \omega_{crit}$ whereas unstable with $\omega < \omega_{crit}$. For example, the particle in water and that in *n*-hexane have the same stability feature. This is a unique property of PQDT, distinguished from PQPT. This observation still holds for the nanoparticles in nano-trap as illustrated in Figure 5. For a nano-particle, the value of b_{DEP} is further increased and as a result, the region of stability is hugely enlarged (see Figure 5(a)), while maintaining the tangent of stability border near (a_{DEP}, q_{DEP}) = (0,0) as zero. It is because the stability features of PQDT are all determined by the first island in the stability chart, and the first island is known to be robust to the change of system parameters for PQPT (Major et al, 2005; Zerbe et al, 1994).

3.3 With fluidic damping, with random motion

Rewriting Eq. (1) with random force as well as fluidic damping,

$$m\frac{d^2x}{dt^2}+\gamma\frac{dx}{dt}-2A_{DEP}\times\left[\mathrm{Re}(f_{CM})+\left|f_{CM}\right|\cos(2\omega t-\phi)\right]x=\sqrt{2k_BT\gamma}W(t) \tag{10}$$

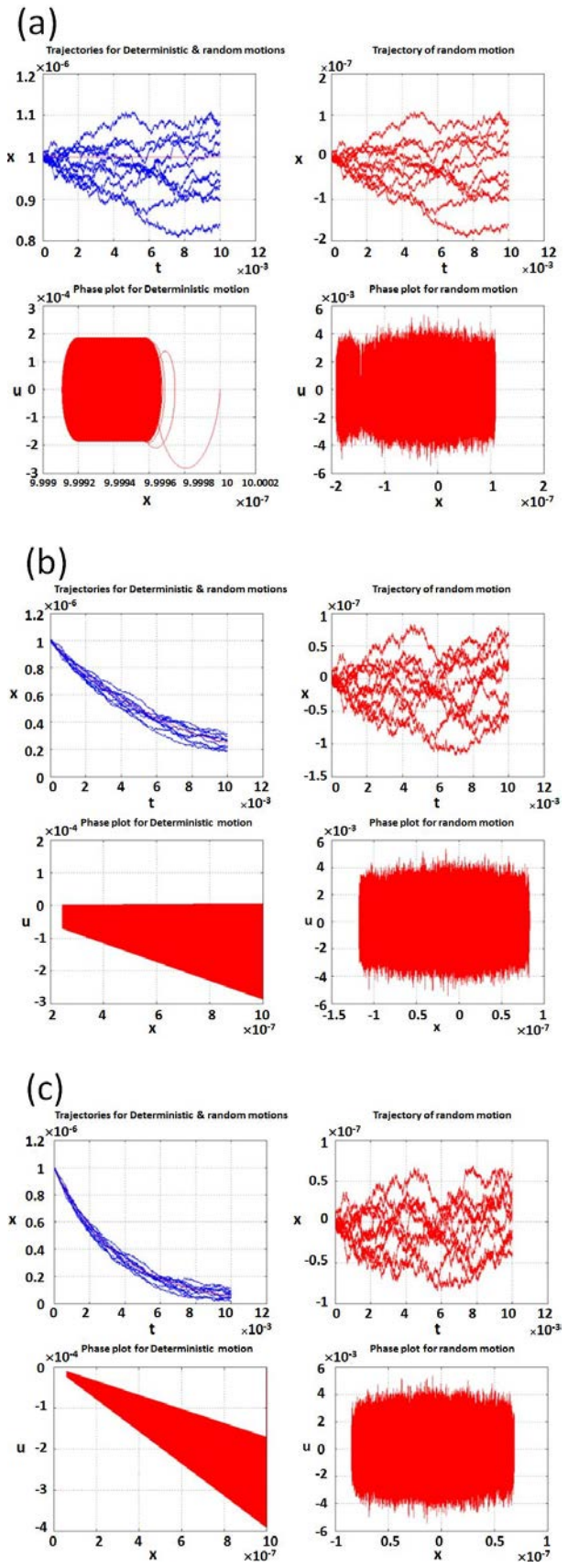

Figure 6. Detailed trajectory and phase plot for micro-particle (r=1μm) in micro-trap (R_0=4μm).: (a) $f=f_{crit}$; (b) $f=1.2f_{crit}$; (c) $f=1.5f_{crit}$.

The particle trajectory $x(t)$ from Eq. (10) consists of the deterministic part, $x_{det}(t)$, and the random oscillation, $x_{ran}(t)$. Two different numerical methods of conventional 4th-order Runge-Kutta method and Euler-Maruyama method (Yuan et al, 2004; Cohen et al, 2012) were applied to numerically compute $x_{det}(t)$ and $x_{ran}(t)$, respectively. A typical trajectory for micro-particle in micro-trap is illustrated in Figure 5(a). The magnitude of random fluctuation was measured by averaging $x_{ran}(t)$ over 10 repetitions with different random seeds. Figure 6 reveals the detailed trajectories and phase plots for micro-particle ($r = 1\ \mu m$) in micro-trap ($r = 4\ \mu m$) at various frequencies of $f = f_{crit}$, $1.2f_{crit}$, and $1.5f_{crit}$. For the stable traps, at long-time limit ($t \rightarrow \infty$) only the random part remains while the deterministic part in the motion vanishes. If the system is not stable, the mean motion itself diverges regardless of the random motion, i.e. the system stability can be determined by the EOS without random motion (Park et al, 2012). The magnitude of random fluctuation at long-time limit, $\sqrt{\langle x_\infty^2 \rangle}$, is estimated from the average over10 repetitions

For the micro-particle in micro-trap, $\sqrt{\langle x_\infty^2 \rangle}$ decreases as 82.8 → 46.7→ 33.6 nm, as ω / ω_{crit} increases as 1.0 → 1.2 → 1.5. The random motion is less than 8% of particle size at most. When only the particle size is reduced by 1/10 (100 nm) with maintaining the trap size, the random fluctuation decreases as 26.2 nm and it remains almost unchanged with the change of frequency (25.8 nm at $\omega = 1.5\omega_{crit}$). However, when the particle with the radius of 100 nm is placed in a nano-trap whose size is R_0 = 400 nm, the random fluctuation is observed as 24.8 nm at $\omega = \omega_{crit}$, which is further reduced as 12.2 and 8.8 nm with increase in frequency as 1.2 and 1.5 ω_{crit}, respectively. Thus, $\sqrt{\langle x_\infty^2 \rangle} / r$ is increased as 24 % at maximum. These observations indicate that the trapping of nano-particle can be successful only with the nano-sized trap, however its random motion becomes comparable to the particle

size. If a nanoparticle is placed in a micro-trap, the random motion will be little controlled by the frequency. The pseudopotential approximation has good agreement with the results from EOS for micro-particle in micro-trap and nano-particle in nano-trap while it overestimates the random motion.

5. Conclusions

In conclusion, in the present study a universal theoretical approach has been developed for the analysis of dynamics of electrical traps such as PQDT and PQPT. The instantaneous formulation for DEP force was employed rather than the ponderomotive expression. This approach leads us to several interesting properties in addition to the reproduction of conventional key properties of PQDT. For example, the stability of PQDT was not affected by the degree of medium viscosity. Also, the quantification of random fluctuation in PQDT was possible. In near future, PQDT is expected to further miniaturize to nanoscale to trap biomolecules (e.g. DNA, RAN, protein, etc.) for single-molecule analysis The current study will be a milestone for such endeavor.

Acknowledgement

This research was supported by Basic Science Research Program through the National Research Foundation of Korea (NRF) funded by the Ministry of Education, Science and Technology (NRF-2012R1A1A1042920).

References

Arnold, S., Folan, L. M., Korn, A., 1993. Optimal Imaging of a Charged Microparticle in an Paul Trap near STP: Stochastic Calculation and Experiment. J. Appl. Phys. 74, 4291-4297.

Berkeland, D. J., Miller, J. D., Bergquist, J. C., Itano, W. M., Wineland, D. J., 1998. Minimization of ion micromotion in a Paul trap. J. Appl. Phys. 83, 5025-5033.

Cohen, D., 2012. On the numerical discretisation of stochastic oscillators. Math. Comput. Simul. 82, 1478-1495.

Gupta, P. K., 2008. Single-molecule DNA sequencing technologies for future genomics research. Trends Biotechnol. 26, 602-611.

Guan, W., Joseph, S., Park, J. H., Krstić, P. S., Reed, M. A., 2011. Paul trapping of charged particles in aqueous solution. Proc. Nat'l Acad. Sci. USA 108, 9326–9330.

Hasegawa, T., Uehara, K., 1995. Dynamics of a single particle in a Paul trap in the presence of the damping force. Appl. Phys. B 61, 159-163.

Hughes, M. P., 2000. AC electrokinetics: applications for nanotechnology. Nanotechnology 11, 124-132.

Hughes, M. P., Morgan, H., 1998. Dielectrophoretic trapping of single sub-micrometre scale bioparticles. J. Phys. D: Appl. Phys. 31, 2205-2010.

Jones, T. B., Wang, K.-L., Yao, D.-J., 2004. Frequency-dependent electromechanics of aqueous liquids: electrowetting and dielectrophoresis. Langmuir 20, 2813-2818.

Kirby, B. J., 2010. Micro- and Nanoscale Fluid Mechanic: Transport in Microfluidic Devices (Cambridge University Press, New York).

Major, F. G., Gheorghe, V. N., Werth, G., 2005. Charged Particle Traps: Physics and Techniques of Charged Particle Field Connement, Springer Series on Atomic, Optical, and Plasma Physics (Springer, Berlin).

Orlin D. V., Sumit G., Dimiter N. P., 2009. Particle-localized AC and DC manipulation and electrokinetics. Annu. Rep. Prog. Chem., Sect. C: Phys. Chem. 105, 213-246.

Park J. H., Krstić, P. S., 2012a. Stability of an Aqueous Quadrupole Micro-Trap. J. Phys.: Condens. Matter 24, 164208.

Park, J. H., Krstić, P. S., 2012b. Thermal Noises in an Aqueous Quadrupole Micro- and Nano-Trap. Nanoscal Res. Lett. 7, 156.

Park, J. H., Guan, W., Reed, M. A., Krstić, P. S., 2012. Tunable Aqueous Virtual Micropore. Small 8, 907-912.

Paul, W., 1990. Electromagnetic traps for

charged and neutral particles. Rev. Mod. Phys. 62, 531-540.

Pethig, R., 2010. Review Article—Dielectrophoresis: Status of the theory, technology, and applications. Biomicrofluidics 4, 022811.

Voldman, J., Braff, R. A., Toner, M., Gray, M. L., Schmidt, M. A., 2001. Holding Forces of Single-Particle Dielectrophoretic Traps. Biophys. J. 80, 531-454.

Voldman, J., 2006. Electrical forces for microscale cell manipulation. Annu. Rev. Biomed. Eng. 8, 425-454.

Walter, N. G., Huang, C.-Y., Manzo, A. J., Sobhy, M. A., 2008. Do-it-yourself guide: How to use the modern single-molecule toolkit. Nature Meth. 5, 475-489.

Washizu, M., Jones, T. J., 1996. Multipolar dielectrophoretic and electrorotation theory. J. Electrostat. 37, 121-134.

Yuan C., Mao, X., 2004. Convergence of the Euler–Maruyama method for stochastic differential equations with Markovian switching. Math. Comput. Simul. 64, 223-235.

Zerbe, C., Jung, P., Hänggi, P., 1994. Brownian Parametric Oscillators. Phys. Rev. E 49, 3626-3635.